Biophysical Journal
Article

Biophysical Society

Vancomycin Reduces Cell Wall Stiffness and Slows Swim Speed of the Lyme Disease Bacterium

Michael W. Harman,[1] Alex E. Hamby,[1] Ross Boltyanskiy,[3] Alexia A. Belperron,[4] Linda K. Bockenstedt,[4] Holger Kress,[3,5] Eric R. Dufresne,[3] and Charles W. Wolgemuth[1,2,*]

[1]Department of Molecular and Cellular Biology and [2]Department of Physics, University of Arizona, Tucson, Arizona; [3]Department of Mechanical Engineering and Materials Science and [4]Department of Internal Medicine, Yale University, New Haven, Connecticut; and [5]Department of Physics, University of Bayreuth, Bayreuth, Bavaria, Germany

ABSTRACT *Borrelia burgdorferi*, the spirochete that causes Lyme disease, is a tick-transmitted pathogen that requires motility to invade and colonize mammalian and tick hosts. These bacteria use a unique undulating flat-wave shape to penetrate and propel themselves through host tissues. Previous mathematical modeling has suggested that the morphology and motility of these spirochetes depends crucially on the flagellar/cell wall stiffness ratio. Here, we test this prediction using the antibiotic vancomycin to weaken the cell wall. We found that low to moderate doses of vancomycin ($\leq$2.0 μg/mL for 24 h) produced small alterations in cell shape and that as the dose was increased, cell speed decreased. Vancomycin concentrations $>$1.0 μg/mL also inhibited cell growth and led to bleb formation on a fraction of the cells. To quantitatively assess how vancomycin affects cell stiffness, we used optical traps to bend unflagellated mutants of *B. burgdorferi*. We found that in the presence of vancomycin, cell wall stiffness gradually decreased over time, with a 40% reduction in the bending stiffness after 36 h. Under the same conditions, the swimming speed of wild-type *B. burgdorferi* slowed by ~15%, with only marginal changes to cell morphology. Interestingly, our biophysical model for the swimming dynamics of *B. burgdorferi* suggested that cell speed should increase with decreasing cell stiffness. We show that this discrepancy can be resolved if the periplasmic volume decreases as the cell wall becomes softer. These results provide a testable hypothesis for how alterations of cell wall stiffness affect periplasmic volume regulation. Furthermore, since motility is crucial to the virulence of *B. burgdorferi*, the results suggest that sublethal doses of antibiotics could negatively impact spirochete survival by impeding their swim speed, thereby enabling their capture and elimination by phagocytes.

INTRODUCTION

Lyme disease is the most prevalent vector-borne disease in the United States, with around 300,000 cases per year (1,2). The disease is caused by infection with the bacterium *Borrelia burgdorferi*, a pathogenic spirochete remarkably adapted to disseminate throughout mammalian hosts (3). Mammals acquire the pathogen when bitten by infected *Ixodes spp* ticks. During tick feeding, the spirochetes migrate from the tick midgut to the tick salivary glands, where saliva deposits *B. burgdorferi* into the dermis of the mammal (4). In the dermis, *B. burgdorferi* replicates and disseminates through the skin. The presence of the bacteria in the dermis produces an immune response that results in skin infiltration of immune cells, leading to erythema migrans, the hallmark skin lesion that is commonly associated with early stages of the disease (5). The bacteria can eventually colonize many organs within the mammal, most notably involving distant skin sites, the heart, the central nervous system, and the joints (5).

The motility of *B. burgdorferi* is essential for the pathogenesis of Lyme disease (6–8). *B. burgdorferi* is able to migrate through a diverse range of environments, such as viscous or viscoelastic fluids (e.g., blood or methylcellulose solutions), the gel-like dermis, or tight junctions between the cells in epithelial or endothelial layers by undulating its entire body as a planar traveling wave. The wave shape of the body is created by wrapping helical flagellar filaments around the cylindrically shaped cell body (Fig. 1, *A* and *B*). In *B. burgdorferi*, 7–11 flagella are anchored into flagellar motors located near both ends of the cell. The flagella reside within the periplasm, the space between the bacterial cell wall and the outer membrane. Confined in this narrow space, the flagella from one end of the cell wrap around the cell

Submitted November 21, 2016, and accepted for publication December 27, 2016.

*Correspondence: wolg@email.arizona.edu

Editor: Dennis Bray.

http://dx.doi.org/10.1016/j.bpj.2016.12.039

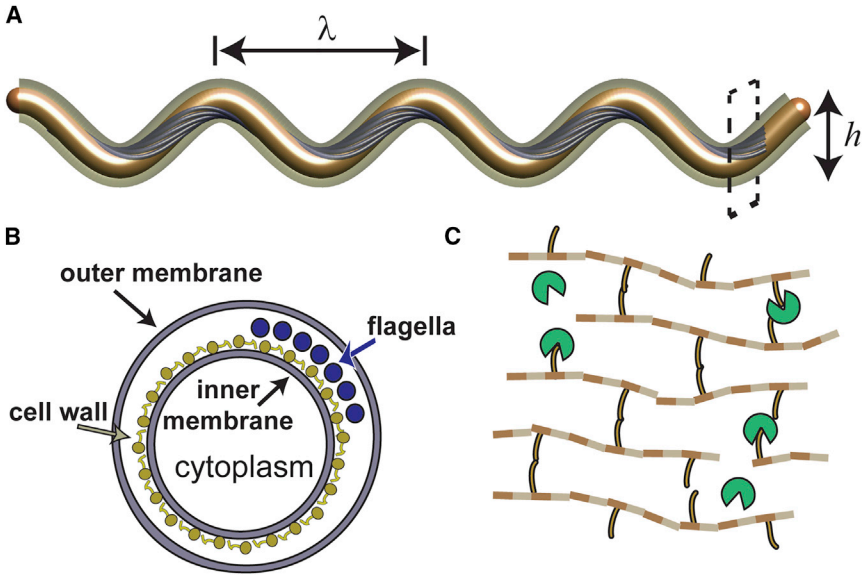

FIGURE 1 (*A*) *B. burgdorferi* has a planar, sinusoidal shape characterized by its wavelength, λ, and amplitude, h. The bacterium creates this shape by wrapping its flagella (*purple*) inside the periplasm, the space between the cell wall (*gold*) and the outer membrane (*gray*). (*B*) A cross section through the cell (corresponding to the black dotted box in (*A*)) shows the location of the flagella with respect to the other cellular components. (*C*) The cell wall in bacteria is made up of glycan strands composed of disaccharide units of GlcNAc-MurNAc (*brown mesh*, with disaccharide subunits *tan* and *brown*, respectively). Peptide chains extend off the MurNAc subunit and can cross-link to neighboring glycan strands. Vancomycin (*green*) binds to the peptides and can prevent cross-linking, which should weaken the cell wall. To see this figure in color, go online.

body toward the other end of the cell (9). Rotation of the flagella within the periplasm causes the waveform to propagate, leading to a traveling wave undulation of the entire body (10). Mathematical modeling has shown that the elastic interaction between the flagella and the cell body is sufficient to generate the planar waveform of the bacteria (11) and that rotation of the flagella will lead to traveling wave deformations, similar to what is observed experimentally (12,13). This mathematical modeling suggests that a key factor in determining the shape and motility of *B. burgdorferi* is the ratio of the flagellar stiffness to that of the cell body. If the cell body is too stiff, then the flagella will not be able to bend the cell into a wave, whereas if the flagella are too stiff, then the cell becomes helical or irregularly shaped. It is likely that the specific shape of *B. burgdorferi* is important in its ability to infect mammals. Consequently, altering the shape and/or stiffness of the bacterium could affect pathogenesis.

The recommended treatment for early-stage Lyme disease is a two- to three-week regimen of oral antibiotics such as doxycyline, amoxicillin, or cefuroxime axetil (14). Although doxycycline acts through inhibition of protein synthesis (15,16), amoxicillin and cefuroxime axetil both interfere with cell wall synthesis (17,18). The cell wall in bacteria is a prime target for antibiotics, since it is the main structural component of the cell and is composed of peptidoglycan, a network of glycan strands connected by peptide cross-links whose molecular constitutents are not found in eukaryotes (Fig. 1 *C*) (19). Disruption of either the cell wall itself or of the proteins that are involved in synthesizing it eventually leads to cell lysis. For example, the broad class of antibiotics known as β-lactams function by mimicking the terminal D-alanyl-D-alanine moieties of the NAM/NAG peptides, allowing them to bind to and inhibit the penicillin-binding proteins (PBPs), which are involved in a large number of peptidoglycan synthetic reactions, including catalyzation of carboxypeptidase, transpeptidase, and endopeptidase reactions and transglycosylation of the N-termini of the glycan strands (20). Many of the β-lactams have demonstrated in vitro activity against *B. burgdorferi*, and antibiotics like penicillin, doxycycline, and ceftriaxone, are known to cause blebbing, granule formation, and a loss of motility in *B. burgdorferi*, as verified by dark-field and electron microscopy (16).

Here, we investigate how the antibiotic vancomycin affects cell stiffness in *B. burgdorferi* to probe the influence of cell wall elasticity on shape and motility. We selected vancomycin over clinically relevant antibiotics like amoxicillin because it specifically blocks peptide cross-linking in the bacterial peptidoglycan by recognizing terminal peptide sequences and blocking their binding site to enzymatic cross-linkers (Fig. 1 *C*), whereas amoxicillin binds the pencillin-binding proteins PBP1a and PBP2, which are involved in cross-linking and glycan strand elongation (21). In addition, vancomycin has previously been shown to be active against *B. burgdorferi* in vitro (22,23). Consistent with this, we show that varying the concentration of vancomycin causes dose-dependent alterations in both the shape and speed of *B. burgdorferi* and that concentrations above 1 μg/mL inhibit growth and lead to cell blebbing. We then used optical traps to bend unflagellated *B. burgdorferi* cells and show that vancomycin produces a weakening of the cell wall that depends on the incubation time. This cell wall weakening leads to minor changes in morphology but a moderate decrease in cell speed. By comparing these results to our previously developed mechanical model for *B. burgdorferi*, we predict that the rotational drag on the flagella will increase as the cell wall becomes stiffer.

MATERIALS AND METHODS

Borrelia culture and vancomycin incubation

All *B. burgdorferi* motility experiments were done using the virulent, green-fluorescent-protein-expressing strain Bb914 (parental strain 297) unless otherwise stated (24). Optical trapping experiments were performed using the B31-derived *flaB* null mutant strain MC-1 (10) (a kind gift from Nyles Charon). Spirochetes were temperature shifted to 37°C in BSK-II medium supplemented with 6% normal rabbit serum (Pel-Freeze Biologicals, Rogers, AK) and harvested in mid-log phase for imaging. Vancomycin was added at a final concentration of 0.5–2.0 μg/mL into exponentially growing *Borrelia* spirochetes and incubated for up to 48 h.

To determine the effect of vancomycin on the growth rate of the cells, we used microscope images to do a visual comparison of the number of cells per field of view between an untreated control sample and cells incubated in vancomycin.

Slide preparation

Chamber slides were made by spreading a thin layer of vacuum grease in the shape of a square the size of a 22 × 22 mm coverslip on microscope slides (Fisher Scientific, Waltham, MA). At each incubation time point (0, 12, 24, and 36 h), 100 μL of *B. burgdorferi* in BSKII were added to the chamber slide, and sealed with a coverslip to reduce environmental fluctuations in the sample. Care was taken to avoid air bubbles between the media and the coverslip.

Imaging

Time-lapse videos of *B. burgdorferi* were acquired at 50 fps using a 40×, 1.2 NA water immersion objective with a CMOS camera (Orca Flash V4.0, Hamamatsu Photonics, Hamamatsu City, Japan) on a Zeiss wide-field epifluorescent microscope (AxioObserver.Z1, Carl Zeiss, Oberkochen, Germany). A minimum of 40 10 s videos were captured for all conditions.

Image processing

An in-house tracking algorithm coded in MATLAB (The MathWorks, Natick, MA) was utilized to extract the center-of-mass position, cell orientation, and amplitude and wavelength of the flat-wave shape from the time-lapse images, as previously described by Harman et al. (13,25). Velocity for spirochetes that remained in the field of view for at least 30 frames was determined using the difference between the center-of-mass positions between subsequent frames. The average translocation velocity over the course of a time series was computed using the power spectrum of the Fourier transform of the velocity, extracting the dominant four modes. These modes were used to reconstruct a smoothed velocity from which the translocation velocity was defined as the maximal amplitude of this smoothed velocity. This maximal amplitude corresponds well to the speed of the cell during constant swimming (i.e., ignoring stops and reversals of direction), which was verified by a number of direct measurements of the speed during continuous swimming. Our analysis of shape and swimming speed excluded cells that were "abnormal." We used three visual criteria to classify spirochetes as being of "abnormal" morphology. These criteria were 1) presence of blebs; 2) absence of a flat-wave appearance, defined by an irregular wavelength/amplitude along the length of the bacterium; and 3) erratic undulation of the body during swimming, characterized by a non-planar waveform that showed rotation and inconsistent undulation between the two ends of the cell. Spirochetes that satisfied any of these conditions were excluded. The respective measurements were averaged across three separate experiments and the mean ± SE was calculated.

Three-point bending assay

Beads. Micromer beads (protein-A-coated 2 μm polystyrene beads) were purchased from Micromod (Rostock, Germany). Each bead has ~58,000 molecules of protein A. Stock beads were at a concentration of 25 mg/mL. Ten microliters of beads were washed with 1 mL of ddH_20 and pelleted for 5 min at 5000 rpm in a microcentrifuge. Beads were then incubated in 100 μL of antibody solution for 1 h or overnight at 4°C with rotation. Monoclonal Osp A antibody C3.78 from hybridoma cell supernatants was used to coat beads (26). After incubation, beads were pelleted and then washed once in phosphate-buffered saline. Beads were vortexed and resuspended in 50 μL phosphate-buffered saline.

Spirochetes were placed into a silicone chamber on a coverslip and incubated with anti-OspA-coated beads. Using holographic optical tweezers (27), beads were attached to a free portion of a *flaB* mutant such that one of the beads was in the middle of the free portion, equidistant from the other two (Fig. 3, *A* and *B*). The middle bead was then translated perpendicular to the symmetry axis of the bacterium in steps of 65–200 nm. The locations of the beads were determined from video images using particle tracking. The forces on the beads were then computed using the differences between the bead locations and the trap positions multiplied by the trap stiffness, where the trap stiffness was determined from fitting the histogram of displacements of a thermally fluctuating bead in the trap to a Gaussian function. The forces exerted on the beads due to bending were recorded at each step, and the force-displacement curves were used to measure the resistance to bending, as described in Results (Eq. 1). A bent configuration of a bacterium is shown in Fig. 3 *B*.

Statistical analysis

To determine whether differences in the amplitudes, wavelengths, speeds, or bending moduli were statistically significant, we first determined whether the data in each data set were normally distributed using the Anderson-Darling test. In all cases, we found that our data were not normally distributed. Therefore, we used a non-parametric Kruskal-Wallis test to determine whether variations in the means of the data were statistically significant. A multiple comparison test was then used to determine the *p*-values between statistically distinct data sets. These statistical tests were carried out in MATLAB using the routines adtest, kruskalwallis, and multcompare.

Mathematical model for the swimming of *B. burgdorferi*

Previous modeling developed a small-amplitude model for the swimming of *B. burgdorferi* (12,13). For the simulations reported here, we have further developed this model to account for large deformations. We used a semi-implicit, finite volume scheme to discretize the equations of motion and solved the equations in MATLAB using a grid of 120 nodes and a time step of 2×10^{-8} s. Details of the mathematical model and our numerical scheme are given in Section S1 of the Supporting Material.

RESULTS AND DISCUSSION

The spirochetes that cause Lyme disease and syphilis, *B. burgdorferi* and *Treponema pallidum*, respectively, are two of the most invasive mammalian pathogens (28). Interestingly, these bacteria have similar morphologies and motility mechanisms, which suggests that the shape of these bacteria may be extremely important to their ability to invade host tissue. A mathematical model has been developed that can explain the shape and movements of both of

these pathogens (11,13,29). Although the model agrees well with the changes in velocity that accompany alterations in the external environment (13), it remains to be shown whether it accurately represents how speed and morphology are affected when the biophysical parameters of the organism are altered. This question is important, since many antibiotics directly affect the cell wall in bacteria and motility is essential for the pathogenesis of Lyme disease (6–8) (and, by inference, is likely essential for syphilis pathogenesis, as well (13)). Therefore, in this study, we sought to systematically examine the effects of vancomycin treatment on cell shape, morphology, and cell wall stiffness (i.e., elastic properties) in *B. burgdorferi*.

Effects of vancomycin on *Borrelia burgdorferi* growth and shape

Microdilution analysis previously measured the in vitro minimal inhibitory concentration (MIC) of vancomycin against *B. burgdorferi* to range from 0.5 to 2.0 μg/mL (22,23). We chose to examine the effects of this range of vancomycin concentrations on exponentially growing bacteria at 24 h with live time-lapse microscopy (Fig. 2 *A–E*). At the higher concentrations of vancomycin ($\geq$1.0 μg/mL), we observed a number of aberrant cells, as identified visually by blebbing, granule formation, and altered morphology. The fraction of these aberrant bacteria in the population increased in a dose-dependent manner (Fig. 2 *F*). For all subsequent analyses, these aberrantly shaped bacteria were excluded.

Using quantitative image analysis similar to that used in (13,25), we examined the impact of weakening the *B. burgdorferi* cell wall on cell morphology (i.e., wavelength and amplitude) and swimming speed. The average wavelength was observed to decrease as the vancomycin concentration was increased from 0 to 1.5 μg/mL (Fig. 2 *G*). In this same range of concentrations, we observed an initial increase in amplitude at 0.5 μg/mL and then a subsequent decrease, as vancomycin concentration was increased to 1.5 μg/mL (Fig. 2 *H*). At a vancomycin concentration of 2.0 μg/mL, we observed an increase in the average amplitude and wavelength; however, cells at this concentration showed large variations in shape, as is exemplified by the large standard deviations in these parameters at this concentration (Fig. 2, *G* and *H*). Swimming speed was observed to consistently decrease with increasing vancomycin concentration, decreasing from 4.92 $\pm$ 0.11 μm/s in untreated cells to 4.32 $\pm$ 0.24 μm/s at 1.5 μg/mL; at 2.0 μg/mL, there was a precipitous drop in swim speed to 1.69 $\pm$ 0.15 μm/s (Fig. 2 *I*). We also found that the percentage of motile cells dropped with increasing vancomycin concentrations, with >90% motile at concentrations of vancomycin $\leq$0.5 μg/mL, 61.3% motile at 1.0 μg/mL, 37.5% motile at 1.5 μg/mL, and 12.5% motile at 2.0 μg/mL.

These results are consistent with the MIC for vancomycin treatment of *B. burgdorferi* being ~1.0 μg/mL. In addition, they show that these concentrations of antibiotic also alter the shape and speed of these spirochetes; however, to determine whether these effects are due to weakening of the cell wall requires that the direct effect of vancomycin on the stiffness of the cell wall be measured.

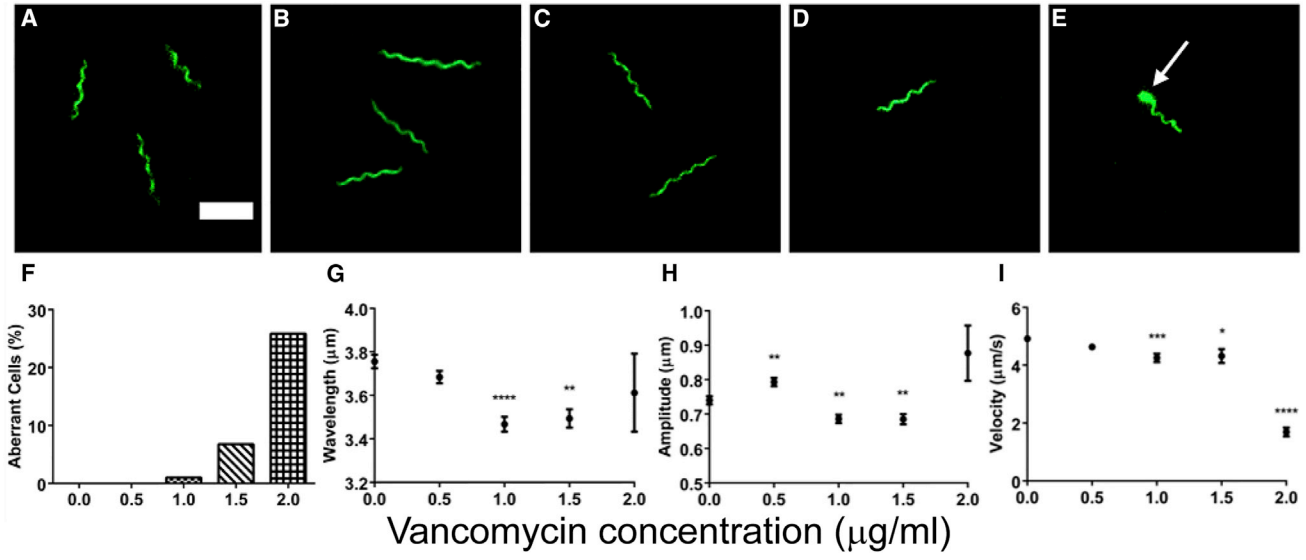

FIGURE 2 Representative images of *B. burgdorferi* incubated for 24 h in vancomycin concentrations of 0 μg/mL (*A*), 0.5 μg/mL (*B*), 1.0 μg/mL (*C*), 1.5 μg/mL (*D*), and 2.0 μg/mL (*E*). Scale bar, 10 μm. Note the steady decrease in density as antibiotic concentration is increased and the presence of blebs (*arrow*) at high concentrations. (*F*) Beginning at vancomycin concentrations of 1.0 μg/mL, there is an increase in the percentage of cells that show blebs and other irregularities. Vancomycin also alters cell shape and speed. (*G–I*) Increasing vancomycin concentration leads to a decrease in the wavelength (*G*) and amplitude (*H*) of the cell shape and also slows cell speed (*I*). The number of cells examined for each concentration are $N = 211$ (0 μg/mL); $N = 285$ (0.5 μg/mL); $N = 124$ (1.0 μg/mL); $N = 96$ (1.5 μg/mL); and $N = 16$ (2.0 μg/mL). A non-parametric Kruskal-Wallis test was used to compare the treated cells to the control group (*$p < 0.05$; **$p < 0.01$; ***$p < 0.001$; ****$p < 0.0001$). To see this figure in color, go online.

Vancomycin weakens the peptidoglygcan cell wall

The stiffness of wild-type cells and individual flagella of *B. burgdorferi* has previously been measured, with individual flagella having a bending modulus of 6.7 ± 3.7 pN μm^2 and intact cells having a modulus of 42 ± 24 pN μm^2 (11). Because the stiffness of wild-type cells is due to the flagella and the cell cylinder (cell wall, inner membrane, and cytoplasm), the cellular bending modulus is some convolution of the bending modulus of the cell cylinder and the flagella. It is therefore not clear how to use this bending modulus to precisely estimate the bending modulus of just the cell cylinder. Therefore, to measure the impact of vancomycin on the stiffness of the cell wall of *B. burgdorferi*, we used a holographic optical trapping system to perform a three-point bending analysis (27) on mutants lacking *flaB*, the gene that encodes the primary protein that forms the flagella (Fig. 3 *A*) (10). To quantify the forces from the optical traps, we adhered 2-μm-diameter polystyrene microspheres coated with mAb to Osp A, the dominant outer surface protein on cultured spirochetes, to three locations along the length of individual bacteria (Fig. 3) (30,31). Holding the two end spheres in place, we then displaced the middle one in a direction roughly perpendicular to the long axis of the cell body (Fig. 3, *B–D*) and measured the force applied at the center bead, *F*, as a function of the displacement of the center microsphere, δ. A characteristic force-displacement curve is shown in Fig. 3 *E*. For small displacements, the curve is nonlinear due to irregularity in the initial locations of the beads, but at larger displacements, the curve becomes linear, as expected from elasticity theory. Treating the bacterium as a solid, cylindrical elastic rod of length *L*, the bending modulus of the cell cylinder, A_c, can then be estimated from the linear part of the force-displacement curve as (32)

$$\delta = \frac{FL^3}{48A_c}. \quad (1)$$

To determine the effect of vancomycin on the stiffness of the cell wall, we wanted to select a concentration at which there would be a measurable effect on cell wall stiffness with minimal effect on other cellular processes. We therefore selected a concentration of 0.5 μg/mL, as the growth rate was not affected at this concentration (Fig. S1) nor did we observe aberrant cell morphologies (Fig. 2 *F*). We then used the three-point bending assay described above to measure the bending modulus as a function of incubation time in vancomycin at 0, 12, 24, and 36 h. At all time points, the force traces looked similar, but there was a decrease in bending modulus at later incubation times. Our control group (the 0 h time point) had a bending modulus of 59 ± 7 pN μm^2 (Fig. 3 *F*), which is the same as what had been previously measured for wild-type *B. burgdorferi*

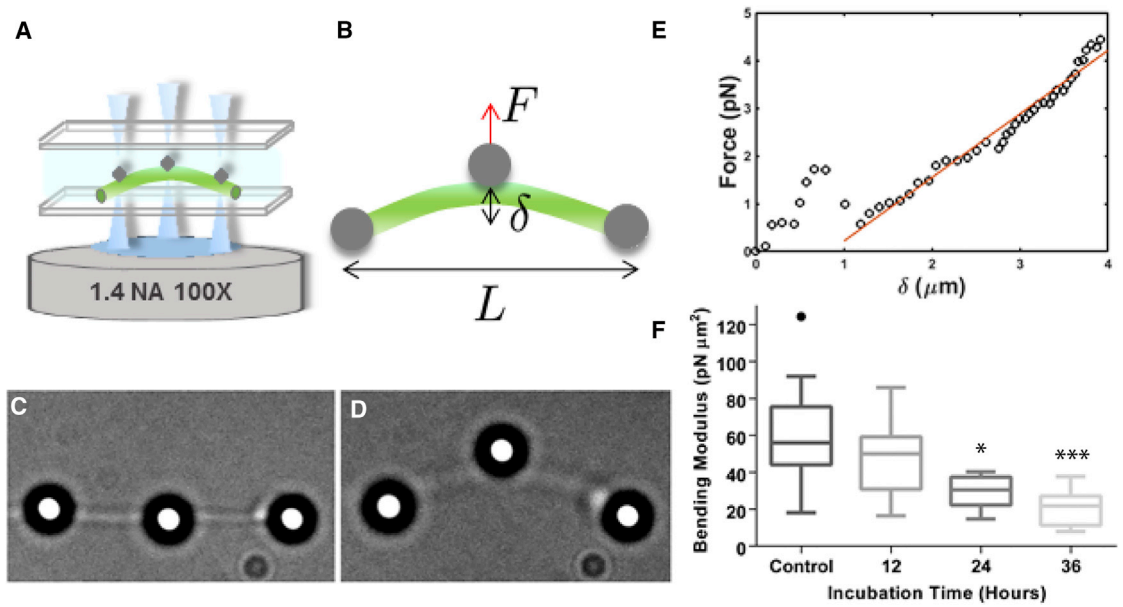

FIGURE 3 (*A* and *B*) We use a holographic optical trapping system to create three trapping beams. Polystyrene microspheres are adhered to the surface of the bacterium at three locations. The two end beads are held fixed in place a distance *L* apart, and the central bead is displaced a distance δ. The force, *F*, that is applied to the central bead is determined from the location of the bead in the trap. (*C–E*) Pre- (*C*) and post-displacement (*D*) images from a characteristic experiment are shown along with a characteristic force-displacement curve (*E*). The bending modulus is determined by fitting a line to the linear part of the curve (*red line*) using Eq. 1. In this experiment, $A_c = 45$ pN μm^2. The beads in (*C*) and (*D*) are 2 μm in diameter. (*F*) The stiffness of the cell wall of flagellaless mutants of *B. burgdorferi* decreases as a function of time when the bacteria are incubated in 0.5 μg/mL of vancomycin for 0, 12, 24, and 36 h. The Kruskal-Wallis test was used to compare the distributions between each time point. Asterisks correspond to the comparison between the treated cells and the control group (*$p < 0.05$; ***$p < 0.001$). To see this figure in color, go online.

(11). After 12 h in 0.5 μg/mL, the bending modulus was found to be 46 $\pm$ 7 pN μm^2, and at 24 and 36 h, the bending modulus decreased further to 29 $\pm$ 3 pN μm^2 and 20 $\pm$ 4 pN μm^2, respectively (Fig. 3 *F*), which amounts to nearly a 60% reduction in bending modulus after 36 h in vancomycin.

These results are interesting for a few reasons. First, the mathematical model for the shape of *B. burgdorferi* that was previously developed suggests that the principal parameter controlling cell shape is the ratio of the flagellar bending modulus to that of the cell cylinder, $\mathcal{A}$ (11). The model also predicts that $\mathcal{A} \sim 1$. Using the bending modulus for the cell cylinder at the zero time point along with the previously measured value of the flagellar bending modulus and the fact that there are 7–11 flagella per cell end (9,33), our data give a value of $\mathcal{A}$ between 0.94 and 1.4. The second interesting aspect of these data is that they suggest that sublethal doses of vancomycin could alter cell morphology and possibly inhibit cell motility. Finally, because we can systematically alter the stiffness of the cell wall, we can then measure the impact of cell wall stiffness on the shape and motility of *B. burgdorferi* for comparison with the predictions from the mathematical model.

Weakened cell wall slows *Borrelia* swim speed

With a well-defined cell wall stiffness as a function of vancomycin incubation time, we could properly assess the swimming dynamics of *B. burgdorferi* as a function of the flagellar/cell wall stiffness ratio. We compared the swimming behavior of single cells treated with vancomycin to that of control cells at the 0 h time point, and to untreated samples at each time point, accounting for any growth-phase-related variations (Fig. 4 *A*; Movie S1). Morphological changes similar to those seen with varying vancomycin concentration were detected with incubation time, with slight shifts in the mean wavelength and amplitude that were inversely proportional to the cell stiffness (Fig. 4, *B* and *C*). The swimming velocity was more severely impacted, decreasing significantly from 4.94 $\pm$ 0.05 to 4.19 $\pm$ 0.09 μm/s (Fig. 4 *H*). To highlight the change in velocity that is produced by the vancomycin, we plotted the percent decrease in velocity relative to untreated cells at the same time points, which showed a drop in speed of ~7% at the 24 h mark and of 15% after 36 h (Fig. 4 *I*).

We previously developed a biomechanical model of the swimming dynamics of *B. burgdorferi* (12,13). To test whether this model could accurately reproduce how changing the cell wall stiffness affects the morphology and motility of *B. burgdorferi*, we simulated the swimming dynamics over a range of cell wall bending moduli from 20 to 60 pN μm^2. Assuming that there were 10 flagella per end, we used a net bending modulus of 70 pN μm^2 for the flagella and a net torque of 20 pN$\cdot\mu$m from the flagellar motors and a rotational drag coefficient of 0.01 pN, both of which are estimated from previous experiments (13). We used the bending moduli computed from our three-point bending experiments to set the bending modulus for the cell wall as a function of time in the vancomycin and compared our simulations to our experimental data. The simulations predicted that the wavelength and amplitude of the bacterium would not change by >5% over the range of bending moduli that we explored, which was consistent with our data (see Fig. 4 *G*). Surprisingly, though, the model predicted that the speed of the cell would increase with decreases in the bending modulus, in direct contrast with our experiments. Although this result may be an indication that vancomycin is affecting more than just the stiffness of the cell wall, another possible explanation for this effect is that as the cell wall becomes weaker, the space between the cell wall and the outer membrane (i.e., the periplasm) decreases in size (see Section S2 in the Supporting Material). If the periplasm is smaller, then there will be increased resistance to rotating the flagella. We tested this hypothesis by assuming that the rotational drag coefficient for the flagella scaled inversely with the cell wall stiffness, $\zeta_\beta = 0.3/A_c$. These simulations still predicted similar small changes in the wavelength and amplitude of the cell that compare well with our experimental observations (Fig. 4 *G*). In addition, the model then predicted that decreasing the bending modulus from 60 to 50 pN μm^2 would produce a small increase in speed, but that further decreases in the bending modulus would reduce the swimming speed in a manner quantitatively similar to what we measured experimentally (Fig. 4 *J*; Movie S2).

The resistance to rotating the flagella in the periplasm is most likely attributable to viscous drag from the periplasmic fluid (34). Because the periplasm is a very narrow space, wall effects can dramatically increase the viscous resistance. Analysis of the low-Reynolds-number dynamics of a cylinder rotating in a narrow gap predicts that the resistive torque is inversely proportional to the square root of the distance from the flagella to the walls of the periplasm (i.e., the cell wall and outer membrane) (35). Cryoelectron microscopy has been used to measure the distance between the inner and outer membranes in *B. burgdorferi*. In the region where the periplasmic flagella reside, the periplasm is 42.3 nm wide (36); the diameter of the flagella is 16 nm (33). If the flagella are perfectly centered within the periplasm, then the distance from the edge of the flagellum to the inner or outer membranes is ~13 nm. Our model predicts that the drag coefficient should increase by a factor of ~2 when the bending modulus of the cell wall decreases from 60 to 25 pN$\cdot\mu$m^2. Since the drag coefficient scales as the square root of the distance, the model suggests that the distance between the flagella and the cell membranes should decrease by a factor of 4, or ~4 nm. Therefore, the model predicts that the periplasmic space in the region of the flagella should decrease to ~24 nm in cells that have been incubated in 0.5 μg/mL of vancomycin for 36 h. This

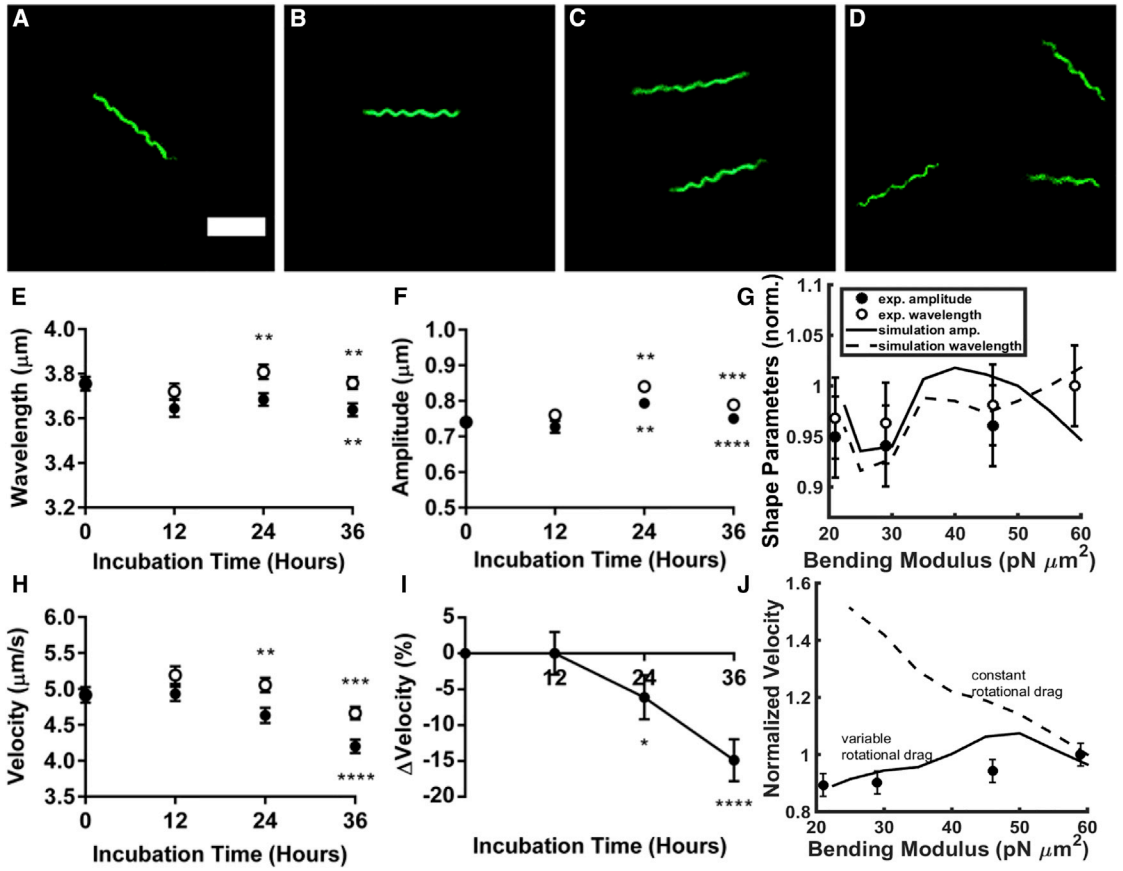

FIGURE 4 Representative images of *B. burgdorferi* incubated in 0.5 μg/mL of vancomycin at 0 (*A*), 12 (*B*), 24 (*C*), and 36 (*D*) h (see also Movie S1). Scale bar, 10 μm. (*E* and *F*) The wavelength and amplitude of vancomycin-treated cells (*solid circles*) decrease by <5% compared to untreated cells (*open circles*). (*G*) The amplitude (*solid circles*) and wavelength (*open circles*) as a function of bending modulus normalized to the amplitude and wavelength of the untreated cells at the same time point. The model predicts similar changes in these quantities (amplitude, *solid line*; wavelength, *dashed line*). Simulation data correspond to the variable rotational drag model. Representative movies from these simulations are shown in Movie S2. (*H*) The speed of the treated cells (*solid circles*) decreases with time in the vancomycin compared to that of untreated cells (*open circles*). (*I*) The percent change in velocity relative to the untreated cells is plotted as a function of time in vancomycin. (*J*) For constant parameters in the model, the model predicts that cell speed should increase with decreasing bending modulus (*dashed line*). However, if the periplasmic space decreases in size as the cell wall becomes softer, then the rotational drag should increase. The model then predicts a similar decrease in speed with decreasing cell bending modulus (*solid line*). In (*E*)–(*J*), all data represent measurements on >200 cells. In (*E*), (*F*), and (*H*), the Kruskal-Wallis test was used to compare the treated and untreated cells at the same time point (*upper asterisks*) and to compare data for treated cells at a specific time point with all data for untreated cells (*lower asterisks*) (*$p < 0.05$; **$p < 0.01$; ***$p < 0.001$; ****$p < 0.0001$). To see this figure in color, go online.

number likely represents an overestimate, as it does not account for the peptidoglycan layer that is also in the periplasm.

The results presented here show that sublethal doses of vancomycin decrease the cell wall stiffness of *B. burgdorferi* in a time-dependent manner and that there is a corresponding decrease in cell speed. In addition, we have provided the first measurement of the cell wall stiffness of a *flaB* mutant of *B. burgdorferi*. These measurements are not confounded by the presence of the flagella, as was the case in earlier reports (11). Interestingly, our new findings place a fairly tight bound on the ratio of the flagellar bending moduli to that of the cell wall. This ratio is observed to be in the range between 0.94 and 1.4, which is in excellent agreement with the previous predictions based on our mechanical model for *B. burgdorferi* (11). Although the model agrees surprisingly well with our measurements of the shape of *B. burgdorferi*, we found that the baseline model does not predict the correct relationship between cell wall stiffness and swimming speed. Although there are many possible explanations for why the model may not make the correct prediction, such as vancomycin having additional effects other than just weakening the cell wall, we showed here that if weakening the cell wall decreases the periplasmic space, then the model can account for the decrease in cell speed with reduction in bending modulus. This prediction can be tested using cryo-EM to measure the periplasmic space in vancomycin-treated cells. If the periplasmic space does not decrease in size, then the model predicts that vancomycin will have an additional effect on the cell that is not being accounted for in the standard mechanism of action for this antibiotic. This result would then suggest novel activity

for this drug, which may be an important finding. Our results also demonstrate that *B. burgdorferi* may have adopted an optimal shape for motility within tissues, and that even low concentrations of antibiotic treatment can significantly inhibit the ability of this bacterium to disseminate through its environment. As motility is an essential aspect in the pathogenesis of Lyme disease (6–8,37), these results suggest that doses of antibiotics below the MIC could enhance the clearing of *B. burgdorferi* by the immune system in patients with Lyme disease.

SUPPORTING MATERIAL

Supporting Materials and Methods, two figures, and two movies are available at http://www.biophysj.org/biophysj/supplemental/S0006-3495(17)30030-9.

AUTHOR CONTRIBUTIONS

A.A.B., L.K.B., H.K., R.B., M.W.H., C.W.W., R.B., and E.R.D. designed the research methodology and wrote the article. M.W.H., R.B., A.E.H., and C.W.W. performed the research. M.W.H., R.B., E.R.D., A.E.H., and C.W.W. analyzed the data.

ACKNOWLEDGMENTS

This research was partially supported by the National Science Foundation (DMS 0920279) and the National Institutes of Health (R01GM072004).

REFERENCES

1. Nelson, C. A., S. Saha, …, P. S. Mead. 2015. Incidence of clinician-diagnosed Lyme disease, United States, 2005–2010. *Emerg. Infect. Dis.* 21:1625–1631.
2. Hinckley, A. F., N. P. Connally, …, P. S. Mead. 2014. Lyme disease testing by large commercial laboratories in the United States. *Clin. Infect. Dis.* 59:676–681.
3. Charon, N. W., A. Cockburn, …, C. W. Wolgemuth. 2012. The unique paradigm of spirochete motility and chemotaxis. *Annu. Rev. Microbiol.* 66:349–370.
4. Ribeiro, J. M. C., T. N. Mather, …, A. Spielman. 1987. Dissemination and salivary delivery of Lyme disease spirochetes in vector ticks (Acari: Ixodidae). *J. Med. Entomol.* 24:201–205.
5. Radolf, J. D., J. C. Salazar, and R. J. Dattwyler. 2010. Lyme disease in humans. *In* Borrelia: Molecular Biology, Host Interaction and Pathogenesis. D. S. Samuels and J. D. Radolf, editors. Caister Academic Press, Norfolk, United Kingdom.
6. Sultan, S. Z., A. Manne, …, M. A. Motaleb. 2013. Motility is crucial for the infectious life cycle of *Borrelia burgdorferi*. *Infect. Immun.* 81:2012–2021.
7. Sultan, S. Z., P. Sekar, …, M. A. Motaleb. 2015. Motor rotation is essential for the formation of the periplasmic flagellar ribbon, cellular morphology, and *Borrelia burgdorferi* persistence within *Ixodes scapularis* tick and murine hosts. *Infect. Immun.* 83:1765–1777.
8. Sze, C. W., K. Zhang, …, C. Li. 2012. *Borrelia burgdorferi* needs chemotaxis to establish infection in mammals and to accomplish its enzootic cycle. *Infect. Immun.* 80:2485–2492.
9. Goldstein, S. F., K. F. Buttle, and N. W. Charon. 1996. Structural analysis of the Leptospiraceae and *Borrelia burgdorferi* by high-voltage electron microscopy. *J. Bacteriol.* 178:6539–6545.
10. Motaleb, M. A., L. Corum, …, N. W. Charon. 2000. *Borrelia burgdorferi* periplasmic flagella have both skeletal and motility functions. *Proc. Natl. Acad. Sci. USA.* 97:10899–10904.
11. Dombrowski, C., W. Kan, …, C. W. Wolgemuth. 2009. The elastic basis for the shape of *Borrelia burgdorferi*. *Biophys. J.* 96:4409–4417.
12. Vig, D. K., and C. W. Wolgemuth. 2012. Swimming dynamics of the Lyme disease spirochete. *Phys. Rev. Lett.* 109:218104.
13. Harman, M., D. K. Vig, …, C. W. Wolgemuth. 2013. Viscous dynamics of Lyme disease and syphilis spirochetes reveal flagellar torque and drag. *Biophys. J.* 105:2273–2280.
14. Wormser, G. P., R. J. Dattwyler, …, R. B. Nadelman. 2006. The clinical assessment, treatment, and prevention of Lyme disease, human granulocytic anaplasmosis, and babesiosis: clinical practice guidelines by the Infectious Diseases Society of America. *Clin. Infect. Dis.* 43:1089–1134.
15. Cunha, B. A., C. M. Sibley, and A. M. Ristuccia. 1982. Doxycycline. *Ther. Drug Monit.* 4:115–135.
16. Kersten, A., C. Poitschek, …, E. Aberer. 1995. Effects of penicillin, ceftriaxone, and doxycycline on morphology of *Borrelia burgdorferi*. *Antimicrob. Agents Chemother.* 39:1127–1133.
17. Weber, D. J., N. E. Tolkoff-Rubin, and R. H. Rubin. 1984. Amoxicillin and potassium clavulanate: an antibiotic combination. Mechanism of action, pharmacokinetics, antimicrobial spectrum, clinical efficacy and adverse effects. *Pharmacotherapy.* 4:122–136.
18. Gold, B., and W. J. Rodriguez. 1983. Cefuroxime: mechanisms of action, antimicrobial activity, pharmacokinetics, clinical applications, adverse reactions and therapeutic indications. *Pharmacotherapy.* 3:82–100.
19. Rogers, H. J., H. R. Perkins, and J. B. Ward. 1980. Microbial Cell Walls and Membranes. Springer, Amsterdam, The Netherlands.
20. Neu, H. C. 1985. Relation of structural properties of β-lactam antibiotics to antibacterial activity. *Am. J. Med.* 79:2–13.
21. Sauvage, E., F. Kerff, …, P. Charlier. 2008. The penicillin-binding proteins: structure and role in peptidoglycan biosynthesis. *FEMS Microbiol. Rev.* 32:234–258.
22. Dever, L. L., J. H. Jorgensen, and A. G. Barbour. 1993. In vitro activity of vancomycin against the spirochete *Borrelia burgdorferi*. *Antimicrob. Agents Chemother.* 37:1115–1121.
23. Hunfeld, K. P., J. Weigand, …, V. Brade. 2001. In vitro activity of mezlocillin, meropenem, aztreonam, vancomycin, teicoplanin, ribostamycin and fusidic acid against *Borrelia burgdorferi*. *Int. J. Antimicrob. Agents.* 17:203–208.
24. Dunham-Ems, S. M., M. J. Caimano, …, J. D. Radolf. 2009. Live imaging reveals a biphasic mode of dissemination of *Borrelia burgdorferi* within ticks. *J. Clin. Invest.* 119:3652–3665.
25. Harman, M. W., S. M. Dunham-Ems, …, C. W. Wolgemuth. 2012. The heterogeneous motility of the Lyme disease spirochete in gelatin mimics dissemination through tissue. *Proc. Natl. Acad. Sci. USA.* 109:3059–3064.
26. Fikrig, E., S. W. Barthold, …, R. A. Flavell. 1990. Protection of mice against the Lyme disease agent by immunizing with recombinant OspA. *Science.* 250:553–556.
27. Mejean, C. O., A. W. Schaefer, …, E. R. Dufresne. 2009. Multiplexed force measurements on live cells with holographic optical tweezers. *Opt. Express.* 17:6209–6217.
28. Wolgemuth, C. W. 2015. Flagellar motility of the pathogenic spirochetes. *Semin. Cell Dev. Biol.* 46:104–112.
29. Vig, D. K., and C. W. Wolgemuth. 2014. Spatiotemporal evolution of erythema migrans, the hallmark rash of Lyme disease. *Biophys. J.* 106:763–768.
30. Radolf, J. D., M. S. Goldberg, …, M. V. Norgard. 1995. Characterization of outer membranes isolated from *Borrelia burgdorferi*, the Lyme disease spirochete. *Infect. Immun.* 63:2154–2163.

31. Charon, N. W., C. W. Lawrence, and S. O'Brien. 1981. Movement of antibody-coated latex beads attached to the spirochete *Leptospira interrogans*. *Proc. Natl. Acad. Sci. USA.* 78:7166–7170.

32. Landau, L. D., and E. M. Lifshitz. 1986. Theory of Elasticity. Butterworth-Heinemann, Oxford, United Kingdom.

33. Hovind-Hougen, K. 1984. Ultrastructure of spirochetes isolated from *Ixodes ricinus* and *Ixodes dammini*. *Yale J. Biol. Med.* 57:543–548.

34. Yang, J., G. Huber, and C. W. Wolgemuth. 2011. Forces and torques on rotating spirochete flagella. *Phys. Rev. Lett.* 107:268101.

35. Yang, J., C. W. Wolgemuth, and G. Huber. 2013. Force and torque on a cylinder rotating in a narrow gap at low Reynolds number: scaling and lubrication analyses. *Phys. Fluids (1994).* 25:51901.

36. Charon, N. W., S. F. Goldstein, …, N. Rowe. 2009. The flat-ribbon configuration of the periplasmic flagella of *Borrelia burgdorferi* and its relationship to motility and morphology. *J. Bacteriol.* 191:600–607.

37. Lin, T., E. B. Troy, …, S. J. Norris. 2014. Transposon mutagenesis as an approach to improved understanding of *Borrelia* pathogenesis and biology. *Front. Cell. Infect. Microbiol.* 4:63.